Numerical Simulation of Wind Pressure Coefficient and Distribution Trend of the Dust Concentration for Parabolic Trough Solar Collector

MingzhiZhao[1], XuZhang[1], XiaomingZhang[2], LuluZou[1], XiaoboKang[1]

[1]School of Energy and Power Engineering, Inner Mongolia University of Technology, Hohhot, China 010051
[2] College of Environmental and Energy Engineering, Beijing University of technology, Beijing, China 100124

zhaomingzhi2020@163.com; zczdzhangxu@163.com

Abstract. Analysis the influence rule of the changing wind angles on the distribution of the pressure coefficient at windward and lee side of collector, and adding the dust particles phase at the completion of the ideal air simulation, simulate the changing rule of the volume fraction of dust around the collector as the change of the attack angle. Under the speed of 10m/s, the conclusion of changing wind angles had no effect on the wind pressure coefficient of the value of windward ,the maximum value range is 0.6-0.7 and the changing wind angles had a great effect on the wind pressure coefficient of the value of leeward, the minimum value range is -0.35—-1.3 and the minimum value is -1.3 at collector angle θ=30 °.When different angles, surface of the collector and the flow field around the dust volume fraction changes a lot, the volume fraction of dust is 2.56 times than the dust entrance at collector angle θ=0°; the volume fraction value significantly angle θ=±60°, its valume fraction is 1.4 times than dust entrance; in the rest of the angles, the volume fraction of collector surface is not much change, only slightly than the exit.

1. Introduction

The country's most abundant resource of solar radiation distributing in most areas of western China, including Inner Mongolia, Gansu, Qinghai, etc. Meanwhile, these areas are suitable for large-scale solar thermal power plants, because the land is flat and open, the cost is low [1]. However, these areas are windy and dusty the whole year. The demonstration project of 50MW pilot solar thermal power plant for Inner Mongolia Da Tang LTD, for example, measured data shows that, the average wind speed of the power station where located in Aragon is about 5m/s. Besides, these places are located in Central Asia sandstorm area which is one of the most active regions of dust activity [2-4]. The special climatic conditions like windy and dusty will have a significant impact on the operation of solar thermal power plants, especially for the solar collector.

At present, the research on wind load is mainly focused on bridges, buildings and other facilities. Lin [5] Studied the wind loads of high-rise buildings at local wind speeds. Bhumralkar C M [6] is the first person to apply numerical simulation to develop a solar collector for wind-resistant research, he used it to carry on the 2-D simulation for the California 100MW solar thermal power station, studied the influence factor on solar thermal power plants including the wind load, the temperature, etc.

Naeeni et al. [7]Simulated the wind load characteristics of a collector under 2-D steady flow field with a 250 kW pilot solar thermal power plant at Shiraz, Iran, using numerical simulation method. According to the above, the wind load of trough collector is mainly carried out by experiments; the simulation mainly focuses on 2-D flow field. This paper focuses on the influence relation of surface pressure and the pattern of sand and dust around the collector by angle of wind approach under 3-D steady flow field.

2. Forces analysis for sand in wind-blown-sand two phase flow

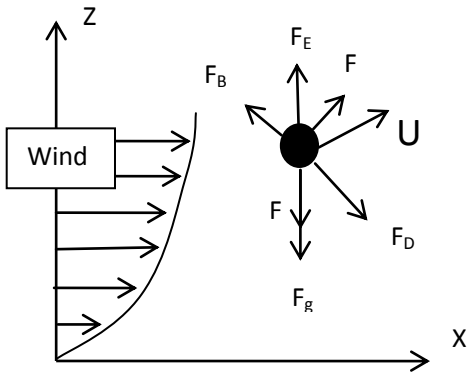

Figure 1. Sketch map of the force of sand in the air

Assuming that the sand is a uniform sphere, CFD predicts the track of a dust by integrating the force-balance equation of the particle. Figure 1 shows the forces analysis for sand in the wind-sand flow. It is assumed that the sand in the XOZ plane for two-dimension motion, the incoming wind speed is given by an exponential wind profile and the direction is along the positive X direction. With the flow in the wind-drift flow, the particle force balance

$$\frac{\mathrm{du_p}}{\mathrm{dt}} = F_D(u - u_p) + \frac{g(\rho_s - \rho)}{\rho_s} + F_x \tag{1}$$

equation has been given where u_p is the track speed, u is the incoming wind speed, R_p is the radius of sand and $\rho_s$is the density, ρ, g are the air density and gravitional acceleration, respectively. F_D is the grabability of sand, is the most important driving force to promote the movement of sand which mainly produced by relative movement between airflow.

In the sand grain balance equation, F_X is including electrostatic force F_E, gravity Fg, Magnuslift force F_M, Saffman lift force F_S and Basset force F_B, etc. This work ignored the influence of electrostatic forces, because there is no regularity of the influence of electrostatic force on sand movement at present.

3. Research Method

3.1Research Content

The windward angle of the collector is changing because the collector needs to track the position of the sun and the wind direction is not constant, so the windward angle is defined as the angle between the incoming wind direction and the plane where the two ends of the parabolic trough collector are connected. These changes cause the flow field around the collector to be different, thus affecting its wind pressure characteristics. In this paper, the surface pressure distribution of it was considered under the windward angle of -90 °, -60 °, -45 °, -30 °, 0 °, 30 °, 45 °, 60 °,90° . And the influence of windward angle on dust settling was studied by adding sand particles. Figure 2 shows the concept map of windward angle.

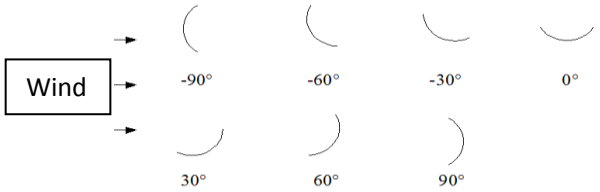

Figure2. Definition of the attack angles

Application of wind engineering research methods, taking the RP3 type trough collector [8] as the most widely used in the world as the model, the CFD software Fluent was used to simulate. The wind pressure at a height of 10 m is taken as a reference value, the mixture model of the FLUENT and the Reynolds time-averaged method were used to simulate the distribution of the wind pressure coefficients of the upwind and leeward side wind collectors with different angles at the wind speeds of 10m/s. And the influence of windward angle on the dust distribution around the collector was studied by adding sand particles.

3.2 Determination of Flow Field and Meshing

3.2.1 Determination of Flow Field. The computational model is established based on the actual model surface and the surrounding flow field. The computational domain size is large enough to ensure that the computational domain boundary does not exert a large influence on the flow field around the collector model, which makes it easier to obtain more accurate simulation results. In the numerical simulation, the blocking rate is used to represent the relationship between the model and the calculated domain size.

$$S = A_b / A_c \quad (2) \qquad (2)$$

Where S is the blocking rate, A_b is the windward area of the model, A_c is the Cross-sectional area of the flow field.

It is pointed out that when the numerical simulation is carried out, the calculation domain blocking rate should not be more than 3% [9] [10]. The dimensions of computational domain of solar collector flow field are show in Table 1.

The computational domain in addition to guarantee the blocking rate, but also need to consider whether the flow field is fully developed while study flow around. Sun [11] suggested that, for the distance from the inlet of the flow field to the windward side of the model is five or six times as the height of the model, the distance from the outlet of the flow filed to the leeward side of the model is seven or nine times as the height of the model, in order to fully develop the flow field.

In this paper, the simulation is a single parabolic trough collector, the design parameters as shown in Table 2. The wind direction is perpendicular to the opening face of the collector, the wind direction angle is constant, whole flow field is symmetrical. In order to simplify the calculation, the computational domain was assumed to be symmetric. So, only half of the simulation was considered.

Table 1. The dimensions of computational domain of solar collector flow field

Altitude （m）	Width （m）	Length of windward （m）	Length of leeward （m）	Bloching rate（%）
43	40	40	120	0.02

Table 2. Design parameter of single parabolic trough reflector

Type of parabolic trough collector	Opening width (mm)	Focal distance （mm）	Concentration ratio	Length (m)	Degree of application
RP3	5770	1710	82	12	Widespread

*3.2.2 Meshing.*A small domain have been built in the area near the collector (as shown in Figure 3) at first, a dense tetrahedron mesh are adopted in this small domain to adapt to the complex flow conditions on surface of the collector and its surrounding, hexahedral mesh are adopted out of the small domain and its mesh quality is sparser than the mall domain.

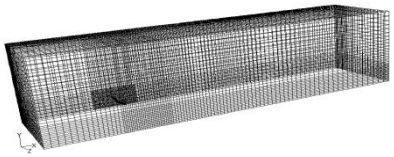

Figure 3.The mesh of computational domain

*3.2.3 Boundary Condition.*Mixture model in eulerian two phases model is adopted in two-phase flow simulation, in order to better simulate the phenomenon of dust settling. The characteristics of sand and sediment concentration are obtained from the actual statistics of sand-dust storm weather in Gansu Province in 1993[12]. Boundary conditions are as follows.

(1) The air fluid is incompressible and the density remains constant.

(2) Dust particles are uniform sphere and the average particle size is $6.44\mu m$.

(3) The particle inlet velocity is equal to the gas flow velocity, and there is no relative slip.

(4) The dust is uniformly distributed with height direction at inlet, the average volume fraction of dust is $3.2\times10^{-5}\%$.

4. Results and discussion

To change the collector angle, the distribution of the windward pressure is large different from the leeward pressure. In the horizontal wind flow, the different vertical plane formed by wind pressure and wind speed on the collector calculated the ratio of the dynamic pressure is called wind pressure coefficient.

4.1 The windward wind pressure coefficient

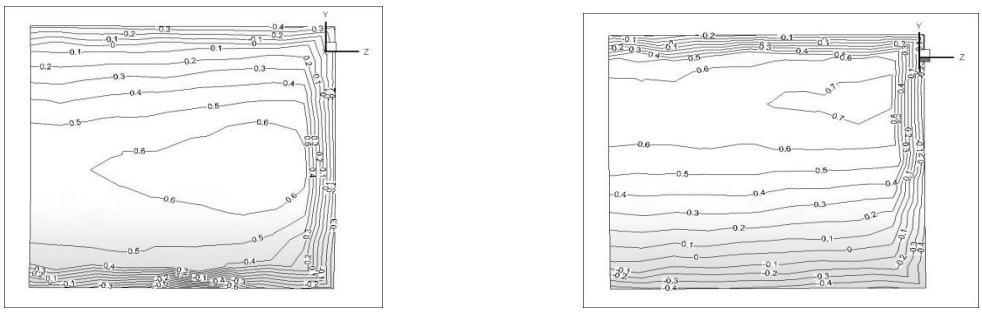

(a)the distribution of Windward pressure coefficient at θ = -90° (b)the distribution of Windward pressure coefficient at θ = -60°

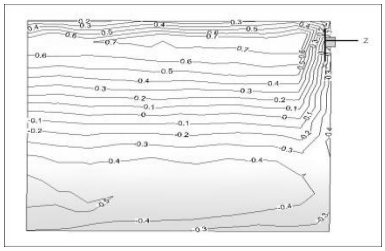

(c)the distribution of Windward pressure coefficient at θ = -30° (d)the distribution of Windwardpressure coefficient at θ = 0°

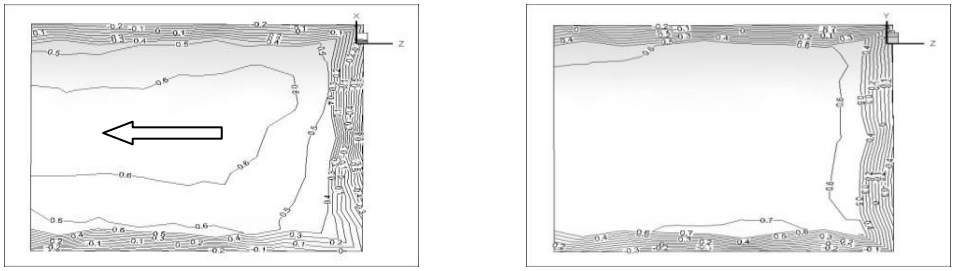

(e)the distribution of Windward pressure coefficient at θ = 30° (f)the distribution of Windward pressure coefficient at θ = 60°

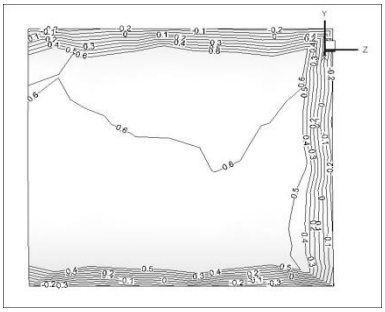

(g).the distribution of Windward pressure coefficient at θ =90°

Figure 4.The distribution of pressure coefficient at windward side of collector

*4.1.1. Flow change.*Base on the special shape of the parabolic trough solar collector, compared with the distribution of wind pressure coefficient for different collector angle from Figure 4 can be seen that changing collector angle has no effect on the windward coefficient (except collector at θ= 0°),the maximum value is 0.6-0.7.No matter how the collector angle changes collectors both ends up and down are always negative pressure, due to the collectors structure is symmetric parabola, when flow impact the surface of collectors ,part of flow rise along the collectors and through it, the other part fall along the collectors and caused eddies. At both ends of the collectors, the wind pressure coefficient of contour are most dense ,due to the distance between collector and ground are closer, the flow is not easy to separate resulting in a greater pressure gradient on the edge.

*4.1.2. Lateral change.*Along the direction of arrow at Figure 4(a), only half of the collector was calculated in the process of simulation, so the windward pressure coefficient of contour are dense in the middle of collector and are sparse at two sides. Maximum value appeared at two sides of the concave surface, is not the center. The cause of this phenomena is that when flow impact the surface of collectors, under the action of resistance the flow is separated two sides of the collector, the flow of

separation and wind blowing are push the surface of collectors cause the wind coefficient rise. So, in the process of design of collector bracket collector to consider the role of wind load on the both end.

*4.1.3.Vertical trend.*Figure 4 (a),(b) ,(c) illustrate that with the collector angle increasing, the position of the wind pressure coefficient maximum value is moving up, the wind pressure coefficient of contour are dense at the head of collector and the minimum value of the bottom of collector is invariably range -0.4—-0.5. With the collector angle increasing, the resistance for flow is decreasing, and the flow of fall along the collector cause eddies between the collector and ground.

When the collector angle at θ=0°, flow approximate flows through the surface and cause a small disturbance around the collector. The wind pressure coefficient maximum value is 0.15 and minimum value is -0.15. The wind pressure distribution on the surface is basic equal at θ＞60°. Only near the edge, due to the effect of separation of the flow, the wind pressure dropped sharply.

4.2 The leeward wind pressure coefficient

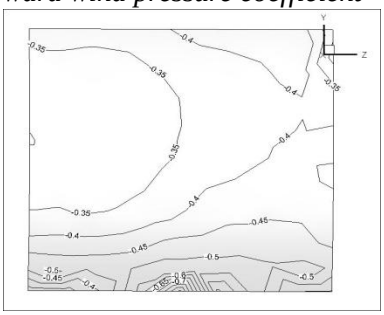

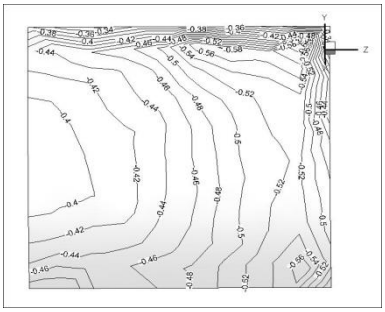

(a).the distribution of leeward pressure coefficient at θ =-90(b).the distribution of leeward pressure coefficient at θ =-60°

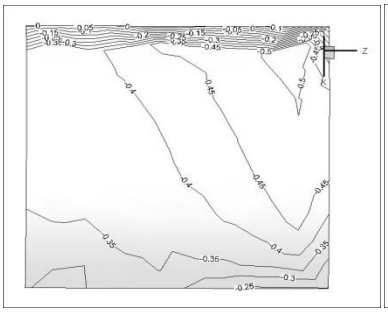

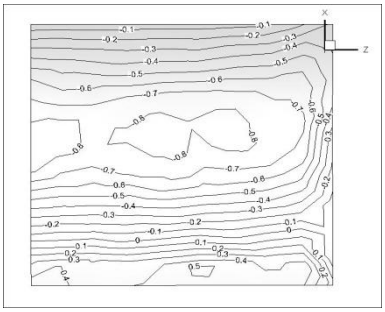

(c).the distribution of leeward pressure coefficient at θ =-30° (d).the distribution of leeward pressure coefficient at θ =0°

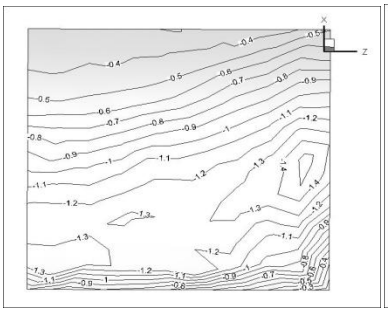

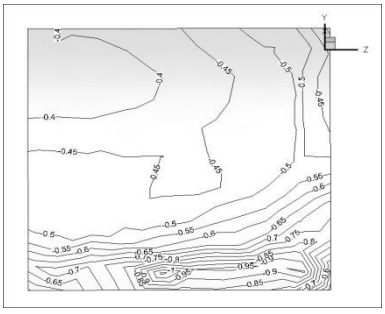

(e).the distribution of leeward pressure coefficient at θ =30° (f).the distribution of leeward pressure coefficient at θ =60°

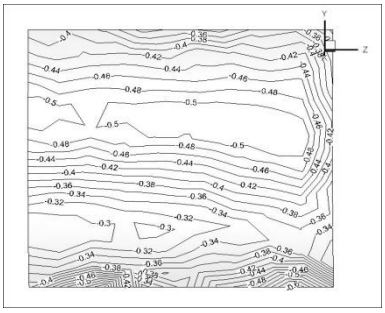

(g).the distribution of leeward pressure coefficient at θ=90°

Figure 5.The distribution of pressure coefficient at lee side of collector

The leeward wind pressure coefficient mainly negative pressure from Figure 5. Windward angle from 90° to 60°, the process of resistance increase, the separation effect of strengthening the collector edge and its maximum leeside wind pressure coefficient is lower. Collector angle θ=0°, the pressure coefficient symmetric distribution on the convex surface. The peaked of leeward wind pressure coefficient is -1.3 at θ= 30°.

4.3 Dust distribution

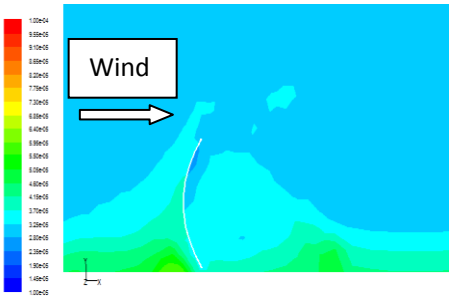

(a).the distribution of the volume fraction

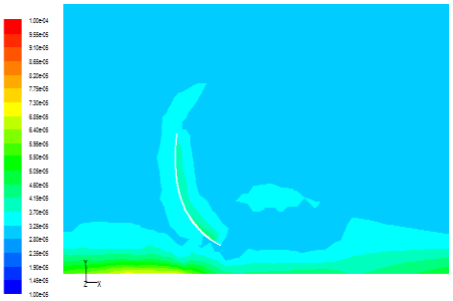

(b).the distribution of the volume fraction of dust around the collector at θ=-90 ℃f dust around the collector at θ=-60 °

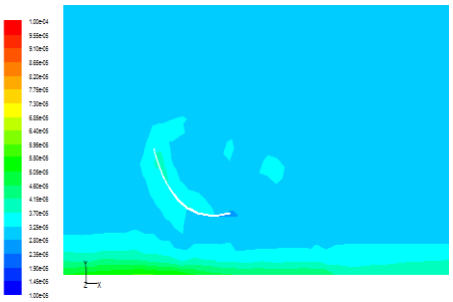

(c).the distribution of the volume fraction

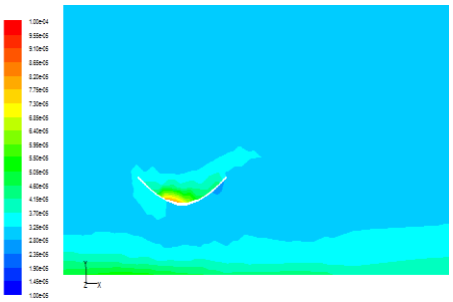

(d).the distribution of the volume fraction of dust around the collector at θ=-30 ℃f dust around the collector at θ=0°

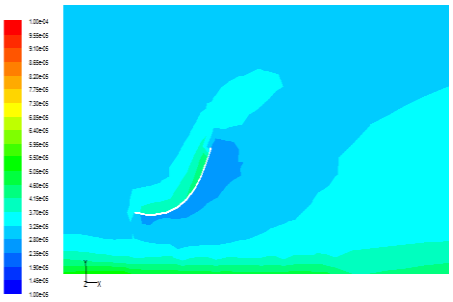

(e).the distribution of the volume fraction

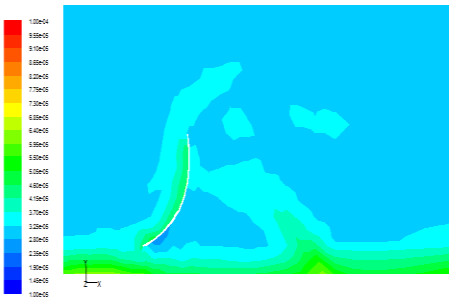

(f).the distribution of the volume fraction of dust around the collector at θ= 30 ℃f dust around the collector at θ= 60 °

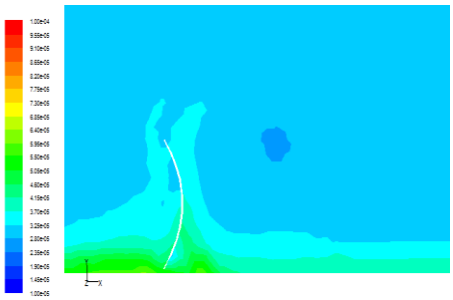

(g).the distribution of the volume fraction of dust around the collector at θ=90°

Figure 6.Volume fraction distribution of dust around collector at different attack angles

Firstly, Figure 6 illustrate the ground of windward are always appear dust-deposition area, because of the collector's resist and sand its own gravity, on the back of the collector also can appear different degree of dust-deposition area. The maximum resistance is collector angle θ=±90°, so the dust-deposition is most obvious and large range at the windward of collector. With the collector angle increase, the dust-deposition area is different. The collector angle from -90°to 0°,the dust-deposition area of the collector leeward is more and more far from the collector, when θ=0°disappear.From θ=0°to θ=90°,the dust-deposition area is appear once again.

What's more, the volume fraction of dust on collector surface is also change with the collector angle change. From Fig.8 the maximum value of the volume fraction of dust is 8.2×10^{-5} % at collector angle θ=0°, and its 2.56 times than the dust entrance. The volume fraction value significantly large angle θ=±60°, its volume fraction is 4.5×10^{-5} % and 1.4 times than dust entrance. In the rest of the angles, the volume fraction of collector surface is not much change, only slightly than the exit.

5. Conclusions

(1) Changing collector angle has no effect on the windward coefficient of the value(except collector at θ=0 ℃), the peaked range is 0.6-0.7 ; no matter how the collector angle changes collectors both ends up and down are always negative pressure; at both ends of the collectors, the wind pressure coefficient of contour are most dense.

(2) The leeward wind pressure coefficient mainly negative pressure. Windward angle from 90 ℃to 60 ℃,the process of resistance increase, the separation effect of strengthening the collector edge and its maximum leeside wind pressure coefficient is lower. Collector angle θ=0 ℃,the pressure coefficient symmetric distribution on the convex surface. The maximum value of leeward wind pressure coefficient is -1.3 at θ=30 ℃.

(3) The volume fraction of dust on collector surface is also change with the collector angle change. From Fig.8 the maximum value of the volume fraction of dust is 8.2×10^{-5} % at collector angle θ=0°, and its 2.56 times than the dust entrance. The volume fraction value significantly large angle

θ=±60°，its valume fraction is 4.5×10^{-5}% and 1.4 times than dust entrance. In the rest of the angles, the volume fraction of collector surface is not much change, only slightly than the exit.

6. Acknowlegement

Supported by National Natural Science Foundation of China (51466011) and Natural Science Foundation of Inner Mongolia (2014MS0511).

7. Reference

[1] Zhao Mingzhi, SongShijin, Zhang Xiaoming 2013 Method research of parabolic trough solar thermal power plant site selection *Renewable Energy Resources***3**(31):18-22.

[2] Qian Zhengan, Song Minhong, Li Wanyuan 2002 Analyses on distributive variation and forecast of sand-dust storms in recent 50 years in north China *Desert Research* **22**(2):106-11.

[3] Su Zhizhu, Dong Guangrong2002Study on the sand-dust storm disaster and prevention countermeasures in northern China *Journal of Shanxi Unversity (Natural Science Edition)***25** (4):361-5.

[4] Wang Tao, Chen Guangting, Qian Zhengan.2001Situation of sand-dust storm and countermeasures in north China *Desert Reserch***21** (4):322-7.

[5] Lin N, Letch Ford G, Tamura Y, Liang B, Nakamura O.2005Characteristics of wind forces acting on tall building *J Wind Eng Ind Aerodyn***93**:217-42.

[6] Bhumralkar C M, Slemmons A J, Nitz K C1981 Numerical study of local regional tmospheric changes caused by a large solar central receiver power plant *Journal of Applied Meteorology***20**: 660-77.

[7] N. Naeeni, M. Yaghoubi2007Analysis of wind flow around a parabolic collector fluid flow *Renewable Energy* **32** (11): 1898-916.

[8] CSPPLAZA Statistical data of the research centre*http://www.cspplaza.com/article-1830-1.html.*

[9] F Baetke, H Werner, H Wengle1990Numerical simulation of turbulent flow over surface-mounted obstacles with sharp edges and corners *Journal of Wind Engineering and IndustriAerodynamics***35**: 129-47.

[10] S A Bekele, H Hangan2002 A comparative investigation of the TTU pressure envelope-Numerical versus laboratory and full scale results. *Wind and Structures* **5** (2-4): 337-46.

[11] Sun Xiaoying, Xu Wei, WuYue 2007 The flow around a blunt body calculation domain research *The 13th national conference of structural wind engineering* Dalian.

[12] Dai XueRong, Shi YuXin, Xue Bin 1995 Granulometric characteristics and significance of the deposits from a recent extraordinary heavy duststorm in Lanzhou, Gansu, northwest China*Journal of lanzhou university(natural science)***31**(4):168—74.